Thermodynamics and Specificity of the Mbp1−DNA Interaction[†]

Lynn Deleeuw, Anna V. Tchernatynskaia,[‡] and Andrew N. Lane*

J. G. Brown Cancer Center, University of Louisville, Louisville, Kentucky 40202, and Department of Chemistry, University of Louisville, Louisville, Kentucky 40208

Received November 27, 2007; Revised Manuscript Received February 17, 2008

ABSTRACT: The DNA binding domain of the yeast transcription factor Mbp1 is a winged helix−turn−helix structure, with an extended DNA binding site involving C-terminal "tail" residues. The thermodynamics of the interaction of the DNA binding domain with its target DNA sequence have been determined using fluorescence anisotropy and calorimetry. The dissociation constant was determined as a function of pH and ionic strength in assessing the relative importance of specific and nonspecific ionic interactions. Mutational analysis of the residues in the binding site was used to determine their contributions to binding. The three tail histidine residues and His 63 in the recognition helix accounted for most of the pH dependence of the DNA binding. The tail histidine residues, along with two previously identified lysine residues, account for a major part of the polyelectrolyte contribution to binding and for the nonspecific affinity of Mbp1 for DNA. Gln 67 was shown to be a very important residue, which interacts in the minor groove of the target DNA. Systematic mutations of the DNA consensus binding sites showed that the CGCG core contributes most to recognition. Isothermal titration calorimetry revealed a strong temperature-dependent enthalpy change, with a ΔC_p of –1.3 kJ mol^{-1} K^{-1}, consistent with a specific binding mode and burial of surface area. Parsing the free energy contributions demonstrates that polyelectrolyte effects account for half of the total free energy at the physiological pH and salt concentration. We present a model for the origin of the sequence specificity and overall affinity of the protein that accounts for the observed thermodynamics.

The Start-specific multimeric transcription complexes MBF (MluI cell cycle box binding factor) and SBF (Swi4/6 cell cycle box binding factor) are central to the control of entry into the cell cycle in *Saccharomyces cerevisiae* (*1*). The Swi6 protein, common to both multimeric complexes, is required for transcriptional activation but possesses no intrinsic DNA binding activity. This activity is supplied by two related proteins, Swi4 and Mbp1[1] (*2, 3*). Thus, Swi6/Swi4 heteromers bind to upstream sequences in the cyclin promoters known as SCBs which exist in multiple copies and have the consensus sequence 5′-CACGAAA-3′ (*2*). Similarly, genes required for DNA replication are regulated by binding of Swi6/Mbp1 heteromers to sequences called MCBs with the consensus sequence 5′-ACGCGTNA-3′ (*4, 5*). Homologous proteins have been identified in fission yeast: Cdc10, Res1/Sct1, and Res2/Pct1 share three regions of sequence similarity with their *S. cerevisiae* counterparts (*6*). The highly conserved N-terminal regions of Swi4, Mbp1, Res1, and Res2 mediate the DNA binding activities of these transcriptional complexes.

The structure of a 124-residue fragment from the N-terminus of Mbp1, Mbp1(124), which comprises the DNA binding domain has been determined by X-ray crystallography (*7, 8*) and NMR (*9*). In the X-ray structures, electron density was observed for only residues 3–100, and the 24 remaining C-terminal residues were disordered. However, deletion analyses and proteolysis protection experiments showed that residues within this C-terminal tail (101–124) are crucial for full DNA binding activity (*10*). The NMR analyses showed that the C-terminal tail folds back onto the N-terminal β-strand of the protein and forms part of the DNA binding surface (*9, 11*). Mutational analysis of the Mbp1 DBD has implicated lysine residues in the tail, as well as the winged helix−turn−helix motif, as being important for DNA binding (*10*).

The DNA binding surface has been mapped using a combination of NMR and computational approaches (*9, 12*). To assess the relative contributions of specific and nonspecific electrostatics and the roles of individual residues in the binding site requires a detailed thermodynamic and mutational analysis. Here we analyze the thermodynamics of binding as a function of pH and ionic strength by fluorescence anisotropy titrations and calorimetry to determine in detail the various contributions to binding (*13, 14*). The results can be rationalized by the structure of the free DNA, and in its complex with the DNA duplex (A. V. Tchernatynskaia et al., unpublished observations).

[†] This work was carried out with support from the Brown Foundation (14.1 T NMR spectrometer), Kentucky Challenge for Excellence (to A.N.L.), and NSF Grant EPS-0447479 for the 18.8 T NMR spectrometer (to R. J. Wittebort).

* To whom correspondence should be addressed: J. G. Brown Cancer Center, University of Louisville, 529 S. Jackson St., Louisville, KY 40202. Telephone: (502) 852-3067. E-mail: anlane01@louisville.edu. Fax: (502) 852-4311.

[‡] Present address: Veterinary Clinical Sciences, College of Veterinary Medicine, University of Minnesota, C339 VMC, 1352 Boyd Ave., St. Paul, MN 55108.

[1] Abbreviations: DBD, DNA binding domain; DSC, differential scanning calorimetry; EMSA, electrophoretic mobility shift assay; Mbp1, Mlu1 binding protein 1; ITC, isothermal titration calorimetry.

10.1021/bi702339q CCC: $40.75
Published on Web 05/21/2008

EXPERIMENTAL PROCEDURES

Materials. (i) Purification of Mbp1 and Variants. The pET 22b-Mbp1 plasmid was transformed into BL21(DE3) competent cells (Novagen) and grown overnight on LB plates with 100 μg/mL ampicillin. One colony was used to inoculate 15 mL of LB medium with 100 μg/mL ampicillin and grown overnight with shaking at 250 rpm and 37 °C. The 15 mL culture was used to inoculate 1 L of LB medium and incubated at 37 °C with shaking until the absorbance at 600 nm (OD_{600}) reached 0.6. The culture was induced with 1.0 mM IPTG and incubated with shaking at 250 rpm for 3 h, and cells were collected by centrifugation at 7000 rpm for 30 min at 4 °C.

The packed cells were lysed using BugBuster (Novagen) containing Benzonase, 1.0 mM PMSF, and 1.0 mM benzamidine. The cell lysate was then sonicated (Branson Digital Sonifier) on ice for 30 s at 55% power every 3 min for seven cycles. After clarification by centrifugation at 15000 rpm and 4 °C for 30 s, the supernatant was loaded directly onto a nickel affinity column (Qiagen), equilibrated, and washed in 100 mM NaCl, 7 mM imidazole, and 20 mM sodium phosphate (pH 7.0). The protein was eluted using a linear imidazole gradient (from 10 to 500 mM).

Mbp1-containing fractions were pooled and buffer-exchanged and concentrated using a Vivaspin membrane concentrator (Sartorius) using 100 mM NaCl and 20 mM sodium phosphate (pH 7.0). The Mbp1 was analyzed by SDS−PAGE and in a DNA band shift binding assay using the DNA duplex sequence d(CTTACGCGTCATTG)• d(CAATGACGCGTAAG).

The Hexahis tag is connected to the Mbp1 protein by a seven-residue linker. Control experiments in which the His tag was removed showed no significant differences in DNA binding or structural characteristics. Previously published NMR data have shown that residues beyond position 122 remain dynamically disordered in the complex with DNA (*15*).

(ii) Protein variants. were made by site-directed mutagenesis using the QuikChange II Site-Directed Mutagenesis Kit (Stratagene). Oligonucleotide primers for the variants were designed with the assistance of the web-based primer design software supported by Stratagene. Variants H20L, H38Q, H63Q, Q67L, Q104L, H117L, H118L, and H119L were chosen according to available structural data, NMR chemical shift perturbations, and cross-saturation experiments that identified likely contacts with the DNA (*7*−*9, 12*). All six histidine residues were mutated to evaluate the role of these residues in specific and nonspecific binding (pH dependence). From the structures, Q67 is expected to interact in the minor groove of the DNA, and Q104 was chosen as a negative control as it should be far from the binding surface (*9*). Mutations were made to residues that occupy comparable space (Leu) and/or preserve hydrogen bonding capacity without charge effects (Gln). The importance of each mutation was determined by determining the pH and ionic strength dependence of the affinity compared to that of the wild-type protein.

The variants were purified and purities analyzed using the same scheme that was used for the wild-type protein. All variants were assessed for conformational integrity and stability by near- and far-UV CD (cf. the Supporting Information).

(iii) DNA Mutations. A non-self-complementary 14-mer DNA having the sequence d(CTT**ACGCGTCA**TTG)• d(CAA**TGACGCGT**AAG) was chemically synthesized and HPLC purified (IDT Inc., Coralville, IA). The bold letters denote the consensus sequence. The two strands were mixed in equal concentrations determined by titration of one strand of known absorbance into the other strand, and the hypochromicity was monitored at 260 nm. The equivalence point of the Job plot was used to mix the stock solutions in the appropriate ratios to produce a 1:1 strand stoichiometry. Stoichiometric duplex formation was verified by polyacrylamide gel electrophoresis. The molar absorbtivity was determined: $\epsilon_{M1} = 114900\ M^{-1}\ cm^{-1}$ and $\epsilon_{M2} = 125900\ M^{-1}\ cm^{-1}$ at 260 nm. The molar absorbtivity of the duplex was determined by digestion with Nuclease P1 using known absorption coefficients of the nucleotides: $\epsilon_{M1M2} = 208600\ M^{-1}\ cm^{-1}$ at 260 nm (*16*). For fluorescence titrations, one strand was 5′ end-labeled with fluorescein (6-FAM), and duplexes were prepared by titration as described above. To assess the relative importance of the DNA base pairs for binding to Mbp1, we systematically varied individual base pairs in the 14-mer consensus DNA sequence (see the Supporting Information).

Methods. (i) Protein−DNA Titrations. Measurements of the affinity of the wild-type and variant Mbp1 for DNA containing the consensus binding site, and point mutations, were carried out carried out as a function of pH and ionic strength to determine the relative contributions of nonspecific electrostatic interactions and specific histidine interactions (cf. ref *10*) to the overall affinity, as follows.

(ii) Fluorescence Measurements. Fluorescence spectra of 5′-fluorescein-labeled DNA were recorded on a Perkin-Elmer LS55 double monochromator fluorimeter equipped with a thermostated stirred cell and polarization. The fluorescein was excited at 495 nm, and emission was recorded at 515 nm. The excitation and emission slits were set to 5 nm. Binding of the protein to the DNA causes an increase in the fluorescence anisotropy because of the increased tumbling time of the DNA in the complex (*17, 18*). Experiments were carried out at 1 μM duplex to avoid complications from dissociation especially at low salt concentrations, and for good sensitivity of the fluorescence anisotropy. Under these conditions, very tight binding appears to be essentially stoichiometric so that only an upper bound to K can be obtained. Control experiments with other dyes, which were less sensitive, showed no significant difference in the thermodynamics.

The anisotropy of the fluorescence was measured as a function of protein and DNA concentration, and the observed anisotropy, r, was analyzed according to

$$r = [r_d + c/d_t(r_F F_C/F_D - r_D)]/[1 + (F_C/F_D - 1)c/d_t] \quad (1)$$

where r_D is the anisotropy of the free DNA, r_F is the anisotropy of the complex, F_C and F_D are the fluorescence intensities of the free and bound DNA, respectively, and c is the concentration of the complex. The latter is given by

$$c = \{(p_t + d_t + K) - \mathrm{sqrt}[(p_t + d_t + K)^2 - 4p_t d_t]\}/2 \quad (2)$$

where p_t and d_t are the total protein and DNA concentrations, respectively, and K is the dissociation constant. When the fluorescence is unperturbed, i.e., $F_C = F_D$, eq 1 reduces to

$$r = r_d + (r_F - r_D)c/d_t$$

Titration curves were analyzed by least-squares using Kaleidagraph (Synergy Software).

(iii) Isothermal Titration Calorimetry. Measurements were taken using a VP ITC microcalorimeter (Microcal). DNA and protein solutions were dialyzed to equilibrium in the appropriate buffers [20 mM sodium phosphate and 100 mM NaCl (pH 7.0)]. Protein at 20 times the concentration of the DNA was titrated into the DNA solution (typically 5–10 μM) in 5–10 μL aliquots. The heat of dilution was subtracted from the raw data, which were then analyzed according to a single-site binding model, which was shown to account well for the data according to the band shift and fluorescence titration assays. Complete binding curves were obtained at three temperatures. ΔC_p was estimated from the dependence of the measured ΔH on temperature as

$$\Delta C_p = \partial \Delta H / \partial T \quad (3)$$

(iv) CD spectra. were recorded on a JASCO J-810 spectropolarimeter with Peltier temperature control. The samples were analyzed in quartz cells with a path length of 0.01 cm for far-UV and a path length of 1 cm for near-UV scans. Far-UV wavelength scans were recorded from 185 to 260 nm, and near-UV wavelength scans were recorded from 250 to 350 nm. The buffer used consisted of 50 mM NaCl and 10 mM sodium phosphate (pH 7.0), and all CD spectra were corrected by subtraction of the buffer background spectrum. The average of five wavelength scans is presented, and results are expressed in terms of mean residue ellipticity (degrees square centimeter per decimole).

The thermal stability of Mbp1 was determined by differential scanning calorimetry (DSC) using a VP-DSC calorimeter (Microcal). Degassed protein at 0.36 mg/mL was introduced into the calorimeter cell in 100 mM NaCl and 20 mM sodium phosphate (pH 7.0). After equilibration, the excess heat capacity was monitored with heating rates of 1 °C/min, scanning from 20 to 90 °C.

(v) Competition EMSA. To determine the affinity of mutant DNA sequences for wild-type Mbp1, we used a competition EMSA approach (cEMSA). Wild-type 14-mer DNA (15 μM) was mixed with an equal concentration of mutant 16-mer, which are resolved on a 20% polyacrylamide gel. Titration of protein into the mixture causes a loss of intensity of the free DNA bands, which can be converted to a relative affinity. Control experiments demonstrated that the length difference had a marginal effect on affinity.

DNA and protein samples in buffer containing 25% glycerol, 50 mM NaCl, and 10 mM sodium phosphate (pH 7.0) were incubated for 30 min, and equal volumes were loaded on the pre-electrophoresis gel. Tracking dye (bromophenol blue) was run in parallel lanes. Electrophoresis for 90 min is sufficient to resolve the DNA bands from one another and from the retarded complexes. The gel was stained with ethidium bromide and imaged using a Bio-Rad digital camera system. The individual band intensities were determined by integration.

For 1:1 binding, the two DNA species compete for free protein according to

$$D + P \overset{K_0}{\leftrightarrow} DP \quad D^* + P \overset{K_1}{\leftrightarrow} D'P \quad (4)$$

where D and D* are the wild-type and mutant DNA oligomers, respectively, and P is Mbp1.

The ratio of the dissociation constants

$$\gamma = K_1/K_0 = dd_p^*/(d^*d_p) \quad (5)$$

In the absence of protein, the free DNA bands represent the total DNA concentration, d_t or d_t^*

$$d_t = d + d_p \quad d_t^* = d^* + d_p^* \quad (6)$$

Hence

$$\gamma = d(d_t^* - d^*)/(d_t - d)d^* \quad (7)$$

The intensities of the free species are determined directly on the gel. The differences $d_t - d$ and $d_t^* - d^*$ were determined for the free band intensities in the absence and presence of protein. Thus, the relative affinity γ is determined.

The free energy loss due to a specific mutation is then

$$\Delta\Delta G = -RT \ln \gamma \quad (8)$$

Given the uncertainties in this procedure, the resulting errors in $\Delta\Delta G$ are in the range of 0.6−1.2 kJ/mol.

NMR spectra were recorded at 14.1 and 18.8 T on Varian Inova spectrometers, at 15 °C as previously described (*15*).

RESULTS

Dependence of Affinity on pH and Ionic Strength: Fluorescence Titrations. Mbp1 binds to the consensus sequence ACGCGTNA (*5*). We have used a non-self-complementary sequence to label either strand separately (see below). The top strand was labeled with fluorescein. When the sample was incorporated into a DNA duplex, the excitation and emission maxima were found to be 495 and 515 nm, respectively. Gel electrophoretic band shift experiments (see below) demonstrated that this sequence is equally as good a target DNA as the self-complementary 12-mer previously described (*10*). To determine the binding affinity, the anisotropy of the fluorescence of the labeled DNA was measured. Figure 1A shows titrations at different pH values at a fixed ionic strength. The anisotropy increased from a low value of ca. 0.05 in the absence of protein, indicating significant internal motion of the fluorophore in the free DNA. At high pH, the anisotropy more than doubled in the presence of saturating concentrations of protein as expected for the increased rotational correlation time of the complex (*11*). The lower saturating anisotropy at lower pH values is consistent with a pH-dependent change in the fluorescence lifetime of the fluorophore. Addition of the protein to the labeled duplex showed no significant shift or change in fluorescence intensity, indicating that the protein does not directly perturb the fluorophore. The affinity of the protein for the DNA was not significantly affected by using a different fluorescence probe or by changing the length of the DNA. Furthermore, NMR experiments showed no evidence of interactions of Mbp1 residues beyond position 122 with the DNA (*11*). Mutational analyses as shown below implicate specific histidine residues in the pH dependence of the affinity. Thus, any interactions between the protein and the label are unlikely to make a significant contribution to the overall thermodynamics. The origins of the pH dependence were tested by mutational analysis (see below).

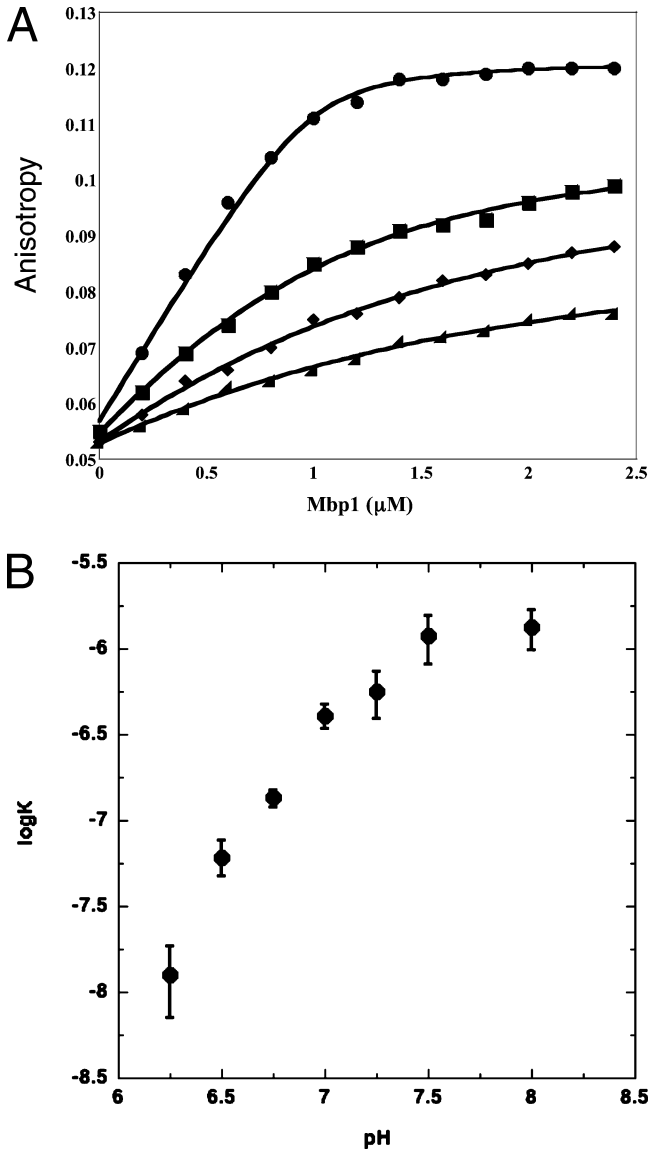

FIGURE 1: Fluorescence anisotropy titration of Mbp1 into labeled DNA and the effect of pH. Titrations were carried out at 25 °C in buffers as described in the text. The buffer consisted of 40 mM sodium phosphate and 200 mM NaCl. (A) Dependence of the fluorescence anisotropy of 5′-fluorescein-labeled DNA (1 μM) on the concentration of Mbp1 at different pH values. The solid line is the nonlinear regression fit to a single site according to eq 1: (●) pH 6.5, (■) 7.0, (◆) 7.5, and (▲) 8.0. The standard deviations of the dissociation constant estimates ranged from 10 to 30% of the best value. The r^2 values ($n = 13$) were all >0.995. (B) Dependence of the apparent dissociation constant on the pH. The dissociation constant was determined by nonlinear regression as described for panel A. The plateau value at high pH defines the affinity of Mbp1 for the protein in which the ionizable groups important for DNA binding are unprotonated.

The Mbp1 molecule contains six histidine residues, four of which are in the putative extended binding surface (and see below). We have therefore measured the pH dependence of the dissociation constant in the range of 6−8.0, as shown in Figure 1B. The apparent pK value for a single protonation site can be assessed according to the scheme.

The apparent Mbp1−DNA dissociation constant is then

$$K = K_1(1 + h/K_a)/(1 + h/K_a') \quad (9)$$

where $h = 10^{-pH}$.

The dissociation constant has reached a plateau by pH 8, which represents the affinity of a deprotonated form of Mbp1 (i.e., for which the groups that titrate in this range are all unprotonated) at this concentration of salt and temperature. The affinity increases approximately 2 orders of magnitude as the pH is decreased from 7 to 6. In the model described above, the value of K_1 would be 1.3 μM. As the affinity increases with a decrease in pH, $pK_a' > pK_a$; i.e., the DNA increases the pK of the ionizable groups. A clear limit to the affinity at low pH could not be reached, but as the minimum observed change in affinity was a factor of 1300, the contribution to the free energy of binding from protonation of these groups is at least 18 kJ/mol at 298 K. The slope of the plot in the pH range from 6 to 7 is 2, which is the lower limit of the number of protons released or absorbed on interacting with the DNA (*14, 19*). At least two ionizable groups must be protonated for maximal affinity.

The DNA binding surface also contains an excess of basic residues (Taylor et al., 1999), which could potentially make electrostatic interactions with the phosphodiester backbone of the DNA. We have determined the influence of ionic strength on K_d at pH 6.5 to evaluate the polyelectrolyte contribution to binding. Log(K_{app}) exhibited a linear dependence on the ionic strength, with a slope, $\partial \log K/\partial \log[Na^+]$, of 4.55. The slope at pH 7.75 was smaller, 3.45; this pH-dependent difference in slope at the two pH values reflects the change in charge on the protein due to ionization of the titratable groups. At 0.14 M sodium, the electrostatic contribution to binding is 22.2 kJ/mol of a total 45.6 kJ/mol. Assuming a thermodynamic value of Ψ of 0.88 (*14, 20, 21*), approximately five ions are released on binding at pH 6.5, and four at pH 7.75. As Figure 1B shows, the ionization is nearly complete by pH 7.75, indicating that approximately four salt-dependent charge interactions between the protein and the DNA do not titrate in the pH range of 6–8. These are likely to be lysine and/or arginine residues (see below).

Isothermal Titration Calorimetry (ITC). The enthalpic contribution to the free energy of binding of wild-type Mbp1 to consensus DNA was determined by ITC. Panels A and B of Figure 2 show a typical titration at pH 7.0, 120 mM Na^+, and 25 °C with a fitted K_d of 0.036 ± 0.006 μM and a ΔH of –40.0 kJ/mol. This is similar to the K_d value of 0.027 ± 0.008 μM, determined by fluorescence titration under identical salt and pH conditions. This is the same as the value estimated by interpolation from the pH and salt dependence (Supporting Information) and indicates that the measured values under these conditions are reasonably accurate. The values of ΔH at 10 and 40 °C were also determined. The thermodynamic parameters are summarized in the Supporting Information. ΔH was strongly temperature-dependent under these buffer conditions; linear regression of ΔH versus absolute temperature gave a slope ΔC_p of –1.3 ± 0.16 kJ mol^{-1} K^{-1}.

Such large changes in heat capacity are characteristic of association-dependent folding and specific binding events (*22–29*) (and see below).

The thermodynamic stability of the protein was determined by DSC, and the protein exhibited a melting temperature of 55 °C (not shown), well above the temperature range used for the thermodynamic analysis. Furthermore, UV melting studies of the DNA showed a melting temperature of 59.0 °C.

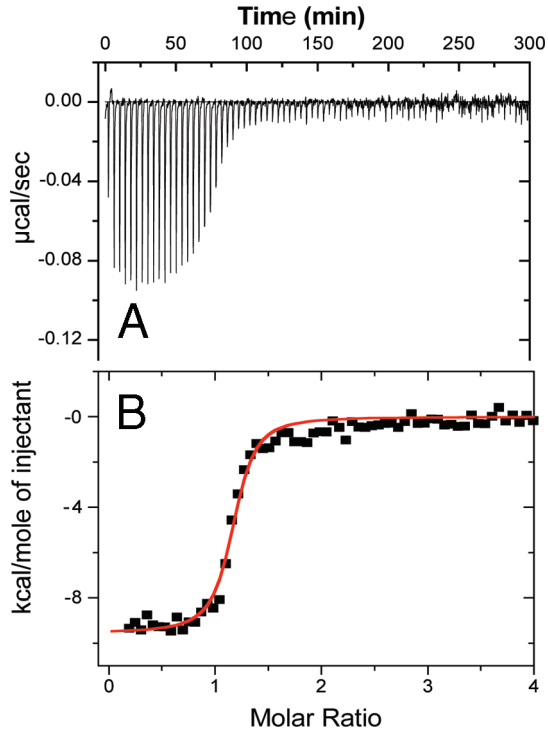

FIGURE 2: Isothermal titration calorimetry. Mbp1 was titrated into DNA [20 mM sodium phosphate, 100 mM NaCl (pH 7.0) buffer] at 25 °C. (A) ITC thermogram of the titration of Mbp1 with DNA. (B) Titration curve. The solid line is the best nonlinear regression fit with an n of 1, a K_d of 0.036 ± 0.006 μM, and a ΔH of –40.0 ± 0.57 kJ/mol.

Mutational Analysis of Mbp1. The binding of the protein variants to the consensus 14-mer DNA was assessed by ITC under standard conditions [20 mM sodium phosphate and 100 mM NaCl (pH 7)] and by fluorescence anisotropy assays as a function of pH and ionic strength.

The pH dependence of the affinity in the pH range of 6−8 and the dependence of the affinity on ionic strength (see above) indicate that several positively charged and ionizable residues are important in the interaction with the DNA. As the affinity increases with a decrease in pH in the range of 6–8, the ionizable residues may be histidines. Mbp1 contains six histidine residues that we have systematically altered to Gln or Leu to determine which ones are most important for the observed pH dependence of the affinity. In addition, there are numerous lysine residues that are potentially important in binding (*10*). Furthermore, Gln 67 is in the wing region and was implicated as a contact residue by chemical shift perturbation and relaxation experiments (*12, 15*). These residues have also been altered to assess their relative contribution to the overall affinity. The location of these residues in the three-dimensional (3D) structure is shown in Figure 3.

In all cases, the variant proteins were shown to be folded at 25 °C by near- and far-UV CD (Supporting Information). The secondary structure predictions showed secondary structures consistent with the NMR structures, and the variations among the protein variants were within the experimental errors of the data. The dependence of the dissociation constant on pH and ionic strength was assessed by measuring the affinity at three different pH values at a fixed ionic strength, and at three different ionic strengths at a fixed pH of 6.5. The value of $\Delta\Delta G$ (wild-type mutant) was calculated for each mutation, and they are plotted in panels A and B of Figure 4.

The least perturbing mutation is that of Q104, as expected because this residue lies on the distal side of the protein from the DNA binding site (cf. Figure 3). The largest perturbations to the free energy under any conditions are from the three histidine residues in the tail region of the protein (H117, H118, and H119), H63, and Q67. Replacement of the three tail histidine residues decreases the free energy of binding more at low pH and low ionic strength, indicting that these must be protonated for optimal binding. Thus, these tail residues contribute at least as much free energy of binding as the previously identified lysine residues (K115 and K121) found in the tail. H63 is in the presumed recognition helix (Figure 4) and makes a substantial contribution to the affinity, even at neutral pH. H20 and H37 are buried in the protein and are remote from the DNA binding site. At neutral pH, replacement of these residues is weakly perturbing (only ca. 2 kJ/mol), though at low pH replacing them with Leu or Gln does diminish the affinity. We presume that these residues are more important for structural integrity than directly in binding. Indeed, the H38L mutation destabilizes the protein, though its observable effect on the tertiary structure itself is quite small. We conclude that the residues mainly responsible for the pH dependence of the affinity are H63, H117, H118, and H119.

Glutamine 67 also contributes substantially to the net affinity, which was predicted for its location and chemical shift perturbation on DNA binding. This residue is located in the wing region of the protein and is presumed to make a contact in the minor groove.

Mutational Analysis of the DNA. Although the consensus binding site has been defined by sequence comparison, we have employed mutational analysis using defined oligonucleotides to determine the relative importance of each residue to the net affinity. We have systematically altered single base pairs as transitions and transversion of bases in the consensus sequence to change the pattern of hydrogen bond donors and acceptors in the grooves. The relative affinity of the mutant for the wild type was determined by a cEMSA as described in Experimental Procedures. Figure 5A shows an example cEMSA titration experiment for two mutant DNAs with wild-type (wt) Mbp1. Increasing the concentration of protein results in a progressive decrease in the amount of free DNA, and the formation of a retarded band. For the GC9-AT9 mutation, the intensity of the wild-type free DNA band disappears at protein concentrations lower than that at which that of the mutant DNA disappears, implying that the mutant binds the protein with lower affinity. As both free bands have disappeared when the Mbp1 concentration equals that of the sum of two DNA species, the stoichiometry is 1:1 for both wt and mutant DNA. In contrast, the TA3/AT mutant and wt DNA show a more similar binding behavior. Thus, this is a convenient method for determining relative affinities even under stoichiometric binding conditions. These data were quantified to provide ratios of dissociation constants as described in Experimental Procedures, from which the difference in the Gibbs energy of binding could be calculated. These $\Delta\Delta G$ values for the various mutants are displayed graphically in Figure 5B. Notably, the core CGCG sequence shows the largest $\Delta\Delta G$ values, and for the most part, these

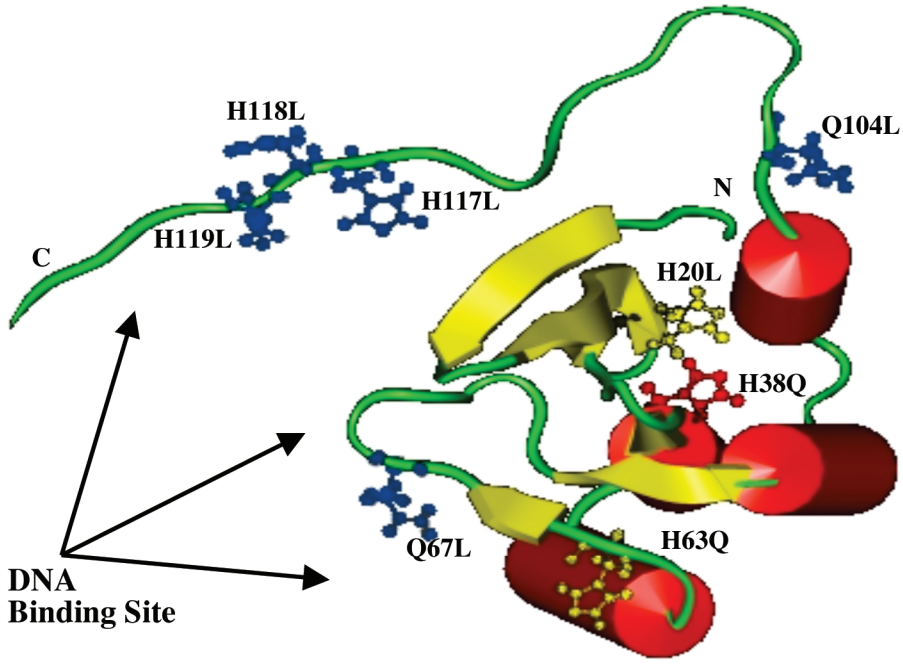

FIGURE 3: Location of protein mutations. Choice of variants and their location in the 3D structure of Mbp1 (structure from ref *9*).

base pairs cannot be substituted. In the flanking regions, although mutations affect the affinity, there is more tolerance for variants. This suggests that the core sequence provides most of the sequence-specific recognition, and the flanking sequences provide overall binding affinity, with an effective site footprint of 10 residues, or one turn of B-DNA.

DISCUSSION

The extended binding surface of Mbp1 contains several basic groups in the recognition helix, as well as in the wing and the C-terminal extension (Figure 3). The thermodynamic results show that the DNA binding domain binds to the 14-mer with moderate affinity (0.04 μM at 25 °C, 120 mM Na^+, and pH 7.0, according to the ITC and fluorescence anisotropy data). Increasing the concentration of monovalent cations causes a decrease in the affinity, indicating the contribution from electrostatic interactions. Similarly, the pH dependence implicates a number of groups (at least two) with pK values below 7 that must be protonated for high-affinity interactions. At pH 8, where the ionizable groups involved in binding are largely deprotonated, the electrostatic contribution to the binding can be estimated by extrapolation of ln(K_d) to an ionic strength of 1 M. The nonelectrostatic contribution to binding is calculated to be 23.4 kJ/mol at 25 °C. This presumably includes the specific interactions. The nonspecific ionic interactions account for 22.2 kJ/mol at 140 mM Na^+ and decrease to 12.2 kJ/mol at 340 mM Na^+. These include the C-terminal lysine residues and presumably other lysine and Arg residues in the binding surface that contribute to the overall positive electrostatic potential distribution (*10*). The enthalpy change is moderate, –40 kJ/mol (of a total ΔG of 42.5 kJ/mol) at 298 K and neutral pH. Overall, the thermodynamic binding characteristics are typical for a specific binding mode (*23, 24, 27*).

Four histidine residues have been identified as being important in DNA binding, one in the recognition helix and three in the C-terminal tail. Two lysine residues in the tail region had been previously identified by mutational analysis, and together, they accounted for a factor of 30 in binding affinity at neutral pH (*10*). We have also positively identified Gln 67 as an important contributor to DNA binding affinity. Removal of the C-terminal tail beyond residue 102 causes a large decrease in DNA binding affinity, on the order of 1000-fold, or a loss of >17 kJ/mol at 298 K (*10*). These data show that the there are five residues in this region that make a significant contribution to the overall binding, but on the basis of the ionic behavior, this is likely to be mainly nonspecific electrostatic interactions. If one assumes that the five residues behave independently, then the overall contribution to the binding energy at pH 7 is 20–25 kJ/mol, which is on the order of the total polyelectrolyte effect.

This suggests that the major role of the C-terminal tail is to provide sufficient overall binding energy, largely in the form of nonspecific electrostatic interactions. The sequence-specific interactions then arise in the recognition helix interacting with the major groove, and the wing region in the minor groove, as exemplified by His 63 and Gln 67.

The polyelectrolyte effect has been parsed from the dependence of the affinity on ionic strength. Other contributions to the overall free energy of binding ΔG_{obs} include the loss of rotational and translational entropy, specific nonelectrostatic interactions, and solvation and conformational changes according to the equation (*14, 30*)

$$\Delta G_{obs} = \Delta G_{hydr} + \Delta G_{r\&t} + \Delta G_{pe} + \Delta G_{conf} + \Delta G_{mol} \quad (10)$$

where ΔG_{conf} is the free energy change due to conformational effects, $\Delta G_{r\&t}$ is the free energy change from loss of rotational and translation freedom on binding, ΔG_{hydr} is the free energy change associated with solvation, ΔG_{pe} is the polyelctrolyte energy, and ΔG_{mol} is the energy change due to differences in molecular parameters. We have determined some terms and estimated others in eq 10, and they are plotted in Figure 6. The hydration term was calculated from the measured heat capacity according to the relation $\Delta G_{hydr} = 80 \pm 10\Delta C_p$ (*28*). For a ΔC_p of –1.28 kJ/mol, we estimate

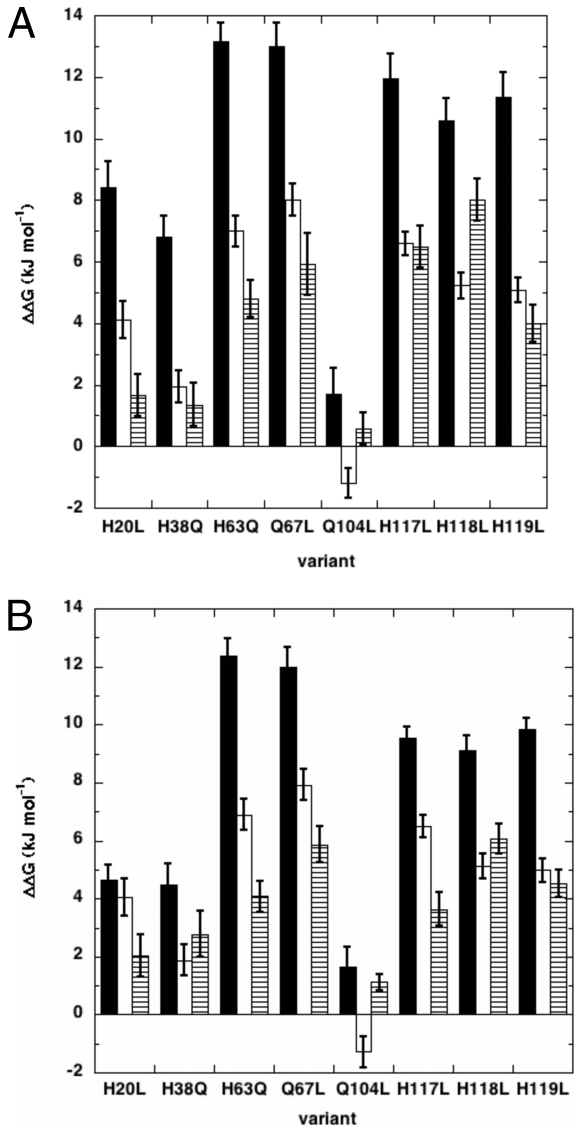

FIGURE 4: Dependence of binding free energy of Mbp1 variants on pH and ionic strength. Free energies of binding were calculated from fitted dissociation constants determined from the fluorescence anisotropy binding assay using the 14 bp DNA consensus sequence duplex as described in Experimental Procedures (cf. Figure 1). The difference in Gibbs energy $\Delta\Delta G$ for variant minus wild type is plotted against variant. (A) pH dependence of $\Delta\Delta G$. The buffer consisted of 40 mM sodium phosphate and 200 mM NaCl: (black) pH 6.0, (white) pH 6.5, and (striped) pH 7.0. (B) NaCl concentration dependence of $\Delta\Delta G$. The buffer consisted of 40 mM sodium phosphate (pH 6.5): (black) 100 mM NaCl, (white) 200 mM NaCl, and (striped) 300 mM NaCl.

a ΔG_{hydr} of –102.4 ± 12.8 kJ/mol. As shown above, the ΔG_{pe} was determined to be –22.2 kJ/mol at 140 mM Na^+. The entropic cost of a decreased level of rotation and translation of the components in the complex is difficult to estimate accurately for numerous reasons. The ranges for $T\Delta S$ quoted in the literature, based on different assumptions and approximations, are on the order of 60 ± 10 kJ/mol (*28*) to lower values of 25–40 kJ/mol (*31*). We have used the high values of 60 ± 10 kJ/mol for this term. The remaining, unfavorable, energy, due to conformational changes in the protein and DNA, is then on the order of 21 ± 24 kJ/mol. If the translational and rotational entropy loss is less than 60 kJ/mol, then the conformational free energy is correspondingly larger.

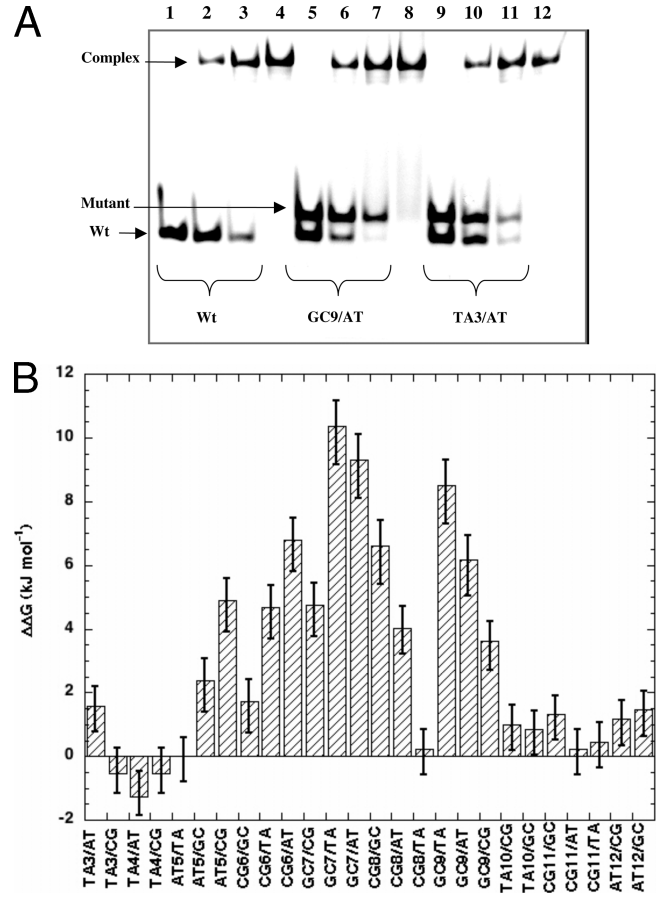

FIGURE 5: Relative binding affinities of DNA single-base pair mutations for wild-type Mbp1. $\Delta\Delta G$ was assessed by a cEMSA. (A) Electrophoresis patterns. Fourteen- and sixteen-base pair DNA duplexes were mixed with increasing concentrations of Mbp1 as described in Experimental Procedures. (B) Relative binding affinities of DNA single-base pair mutations for Mbp1. $\Delta\Delta G$ was determined by a cEMSA according to eq 7 in the text.

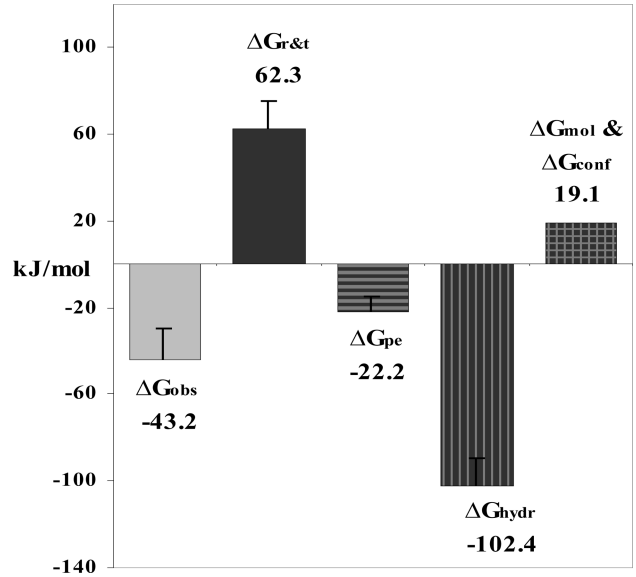

FIGURE 6: Parsing the free energy of binding of Mbp1 to DNA. The free energy was parsed into several terms according to eq 10 as described in the text. Error bars are either those derived from experiment or estimates due to uncertainty in literature values.

We have observed changes in the conformation of the DNA moiety on binding Mbp1, and also in the protein on DNA binding, especially near the wing and in the C-terminal

tail region (*10, 11*). The influence of conformational selection, i.e., a decrease in the conformational space available on complex formation, has been described in detail (*14, 28*). At higher temperatures, ΔS is less favorable as more states become accessible in the free protein and free DNA, and the energy required to distort the DNA is relatively small. At low temperatures, the energy needed to distort the DNA is large compared with the energy obtained from binding, leading to a small observed enthalpy change; overall, the heat capacity change is negative, reflecting both the conformational selection of states within the protein and the temperature-dependent enthalpic costs of DNA distortion.

ACKNOWLEDGMENT

This work represents partial fulfillment of requirements for a M.S. degree for L.D. at the University of Louisville. We thank Drs. J. B. Chaires and N. Garbett for critical suggestions and comments about the work.

SUPPORTING INFORMATION AVAILABLE

Tables of mutations, thermodynamic data, and figures of protein integrity. This material is available free of charge via the Internet at http://pubs.acs.org.

REFERENCES

1. Bean, J. M., Siggia, E. D., and Cross, F. R. (2005) High functional overlap between MluI cell-cycle box binding factor and Swi4/6 cell-cycle box binding factor in the G1/S transcriptional program in *Saccharomyces cerevisiae*. *Genetics 171*, 49–61.
2. Primig, M., Sockanathan, S., Auer, H., and Nasmyth, K. (1992) Anatomy of a Transcription Factor Important for the Start of the Cell-Cycle in *Saccharomyces cerevisiae*. *Nature 358*, 593–597.
3. Koch, C., Moll, T., Neuberg, M., Ahorn, H., and Nasmyth, K. (1993) A Role for the Transcription Factors Mbp1 and Swi4 in Progression from G1 to S-Phase. *Science 261*, 1551–1557.
4. McIntosh, E. M. (1993) Mcb Elements and the Regulation of DNA-Replication Genes in Yeast. *Curr. Genet. 24*, 185–192.
5. McIntosh, E. M., Atkinson, T., Storms, R. K., and Smith, M. (1991) Characterization of a Short, Cis-Acting DNA-Sequence Which Conveys Cell-Cycle Stage-Dependent Transcription in *Saccharomyces cerevisiae*. *Mol. Cell. Biol. 11*, 329–337.
6. Lowndes, N. F., Johnson, A. L., Breeden, L., and Johnston, L. H. (1992) Swi6 Protein Is Required for Transcription of the Periodically Expressed DNA-Synthesis Genes in Budding Yeast. *Nature 357*, 505–508.
7. Taylor, I. A., Treiber, M. K., Olivi, L., and Smerdon, S. J. (1997) The X-ray structure of the DNA-binding domain from the *Saccharomyces cerevisiae* cell-cycle transcription factor Mbp1 at 2.1 angstrom resolution. *J. Mol. Biol. 272*, 1–8.
8. Xu, R. M., Koch, C., Liu, Y., Horton, J. R., Knapp, D., Nasmyth, K., and Cheng, X. D. (1997) Crystal structure of the DNA-binding domain of Mbp1, a transcription factor important in cell-cycle control of DNA synthesis. *Structure 5*, 349–358.
9. Nair, M., McIntosh, P. B., Frenkiel, T. A., Kelly, G., Taylor, I. A., Smerdon, S. J., and Lane, A. N. (2003) NMR structure of the DNA-binding domain of the cell cycle protein Mbp1 from *Saccharomyces cerevisiae*. *Biochemistry 42*, 1266–1273.
10. Taylor, I. A., McIntosh, P. B., Pala, P., Treiber, M. K., Howell, S., Lane, A. N., and Smerdon, S. J. (2000) Characterization of the DNA-binding domains from the yeast cell-cycle transcription factors Mbp1 and Swi4. *Biochemistry 39*, 3943–3954.
11. McIntosh, P. B., Taylor, I. A., Frenkiel, T. A., Smerdon, S. J., and Lane, A. N. (2000) The influence of DNA binding on the backbone dynamics of the yeast cell-cycle protein Mbp1. *J. Biomol. NMR 16*, 183–196.
12. Lane, A. N., Kelly, G., Ramos, A., and Frenkiel, T. A. (2001) Determining binding sites in protein-nucleic acid complexes by cross-saturation. *J. Biomol. NMR 21*, 127–139.
13. Haq, I., Jenkins, T. C., Chowdhry, B. Z., Ren, J. S., and Chaires, J. B. (2000) Parsing free energies of drug-DNA interactions. *Methods Enzymol. 323*, 373–405.
14. Lane, A. N., and Jenkins, T. C. (2000) Thermodynamics of nucleic acids and their interactions with ligands. *Q. Rev. Biophys. 33*, 255–306.
15. McIntosh, P. B., Taylor, I. A., Frenkiel, T. A., Smerdon, S. J., and Lane, A. N. (2000) The influence of DNA binding on the backbone dynamics of the yeast cell-cycle protein Mbp1*. *J. Biomol. NMR 16*, 183–196.
16. Cavaluzzi, M. J., and Borer, P. N. (2004) Revised UV extinction coefficients for nucleoside-5′-monophosphates and unpaired DNA and RNA. *Nucleic Acids Res. 32*, e13.
17. Grillo, A. O., Brown, M. P., and Royer, C. A. (1999) Probing the physical basis for trp repressor-operator recognition. *J. Mol. Biol. 287*, 539–554.
18. Reedstrom, R. J., Brown, M. P., Grillo, A., Roen, D., and Royer, C. A. (1997) Affinity and specificity of trp repressor−DNA interactions studied with fluorescent oligonucleotides. *J. Mol. Biol. 273*, 572–585.
19. Wyman, J. J. (1964) Linked functions and reciprocal effects in hemoglobin: A second look. *Adv. Protein Chem. 19*, 223–315.
20. Anderson, C. F., and Record, M. T. (1995) Salt Nucleic-Acid Interactions. *Annu. Rev. Phys. Chem. 46*, 657–700.
21. Record, M. T., Jr., Anderson, C. F., and Lohman, T. M. (1978) Thermodynamic analysis of ion effects on the binding and conformatinal equilbria of protein and nucleic acids. *Q. Rev. Biophys. 11*, 103–178.
22. Poon, G. M. K., Gross, P., and Macgregor, R. B. (2002) The sequence-specific association of the ETS domain of murine PU.1 with DNA exhibits unusual energetics. *Biochemistry 41*, 2361–2371.
23. Jen-Jacobson, L., Engler, L. E., Ames, J. T., Kurpiewski, M. R., and Grigorescu, A. (2000) Thermodynamic parameters of specific and nonspecific protein-DNA binding. *Supramol. Chem. 12*, 143.
24. Lundback, T., Chang, J. F., Phillips, K., Luisi, B., and Ladbury, J. E. (2000) Characterization of sequence-specific DNA binding by the transcription factor Oct-1. *Biochemistry 39*, 7570–7579.
25. Oda, N., and Nakamura, H. (2000) Thermodynamic and kinetic analyses for understanding sequence-specific DNA recognition. *Genes Cells 5*, 319–326.
26. Oda, M., Furukawa, K., Ogata, K., Sarai, A., and Nakamura, H. (1998) Thermodynamics of specific and non-specific DNA binding by the c-Myb DNA-binding domain. *J. Mol. Biol. 276*, 571–590.
27. Lundback, T., and Hard, T. (1996) Sequence-specific DNA-binding dominated by dehydration. *Proc. Natl. Acad. Sci. U.S.A. 93*, 4754–4759.
28. Spolar, R. S., and Record, M. T. (1994) Coupling of Local Folding to Site-Specific Binding of Proteins to DNA. *Science 263*, 777–784.
29. Jin, L. H., Yang, J., and Carey, J. (1993) Thermodynamics of Ligand-Binding to Trp Repressor. *Biochemistry 32*, 7302–7309.
30. Chaires, J. B. (1997) Energetics of drug-DNA interactions. *Biopolymers 44*, 201–215.
31. Horton, N., and Lewis, M. (1992) Calculation of the Free-Energy of Association for Protein Complexes. *Protein Sci. 1*, 169–181.

BI702339Q